**Nationaal Lucht- en Ruimtevaartlaboratorium**
National Aerospace Laboratory NLR

NLR-TP-99133

# Sound diffraction by the splitter of a turbofan engine

R.J. Nijboer and P. Sijtsma

**Nationaal Lucht- en Ruimtevaartlaboratorium**

National Aerospace Laboratory NLR

NLR-TP-99133

# Sound diffraction by the splitter of a turbofan engine

R.J. Nijboer and P. Sijtsma

This report is based on a presentation to be held on the sixth International Congress on Sound and Vibration, Lyngby, Denmark.

The sixth International Congress on Sound and Vibration has granted NLR permission to publish this report.

Division: Fluid Dynamics
Issued: 17 March 1999
Classification of title: Unclassified

## Contents



2 Tables
4 Figures

(12 pages in total)

# SOUND DIFFRACTION BY THE SPLITTER OF A TURBOFAN ENGINE

R.J. Nijboer and P. Sijtsma
National Aerospace Laboratory NLR, P.O. Box 153, 8300 AD Emmeloord,
The Netherlands

## ABSTRACT

The diffraction of noise by a splitter that separates the bypass flow from the flow into the core engine of a turbofan engine is analysed. By using the Wiener-Hopf technique a closed form solution is found. This solution is then analysed numerically and results on single modes are discussed. It is demonstrated that acoustic modes of high radial order undergo more effect of diffraction than low order radial modes. Also the low order radial modes originating from the inner stator row (Engine Section Stator; ESS) seem to be more affected by diffraction than those coming from the outer stator row (Outlet Guide Vanes; OGV). Due to diffraction a small part of the noise is reflected or deflected from ESS to OGV (or from OGV to ESS). However, the largest part of the noise propagates towards the fan. The major effect of diffraction is a redistribution of the noise over radial acoustic modes.

## INTRODUCTION

The duct of a turbofan engine downstream of the fan splits into a bypass duct and an engine duct, see figure 1. Since the fan is driven, swirl is added to the airflow in the ducts. In order to take this swirl out of the airflow and recover the energy from the swirl, stators are placed in the engine duct and in the bypass duct. Rotor wakes interact with the stator vanes and thus generate sound. Part of this rotor/stator interaction noise travels back towards the fan, which partly reflects it and partly transmits it.

Sound generated by the interaction between the rotor and the bypass stator row (Outlet Guide Vanes; OGV) and radiating towards the fan is usually modelled with neglect of the splitter. If sound generated at the inner stator row (Engine Section Stators; ESS) is considered, the splitter can hardly be ignored. For that purpose, a model for sound diffraction at the splitter is needed. The theory of diffraction by the splitter is reported here. With such a theory, better input can be generated for rotor blockage calculations (Ref. 1) and liner optimisation.

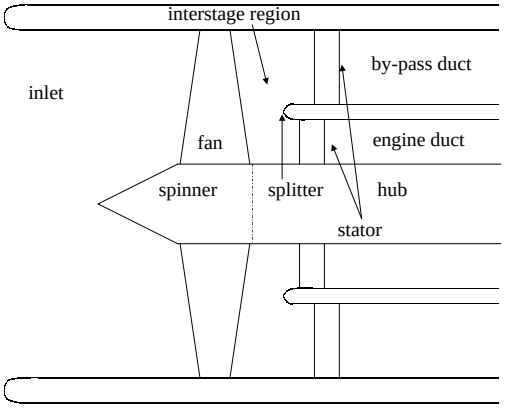


*Fig. 1 Schematic view of part of a turbofan engine*

In the analysis a number of assumptions is made. First of all, a duct with constant, circular cross-section is assumed. Furthermore, the background flow is uniform, subsonic and does not contain swirl or boundary layers. Finally, the splitter is assumed to be infinitely thin. The analysis is restricted to the interstage region of the engine. This region is divided into three sub-regions, for each of which the radial eigenfunctions are calculated. The diffraction problem in the interstage region is discussed, after which the problem is solved using the Wiener-Hopf technique (Ref. 2). The most crucial part of this technique is the splitting of the so-called kernel function. When this is done appropriately, the solution to the diffraction problem is found in closed form. The solution is then analysed numerically for single modes.

## EIGENSOLUTIONS

In the analysis to follow, the physical quantities are made dimensionless using the air density, the speed of sound and the tip radius of the fan. The interstage region of a turbofan engine (Fig. 1) is modelled by a cylindrical pipe. The region directly downstream of the fan ranges from hub to outer radius ($h \le r \le 1$; region I). The duct is split into a region from hub to splitter ($h \le r \le s$; region II), and a region from splitter to outer radius ($s \le r \le 1$; region III), see figure 2. The airflow is assumed to contain no swirl, which is a simplification of the physical problem. The flow velocity, which is assumed to point in the $x$ direction, is characterised by the Mach number $M$, which is assumed to be constant, positive, and less than 1. The splitter is assumed to be infinitely thin and semi-infinite in positive $x$-direction, starting at $x=0$.

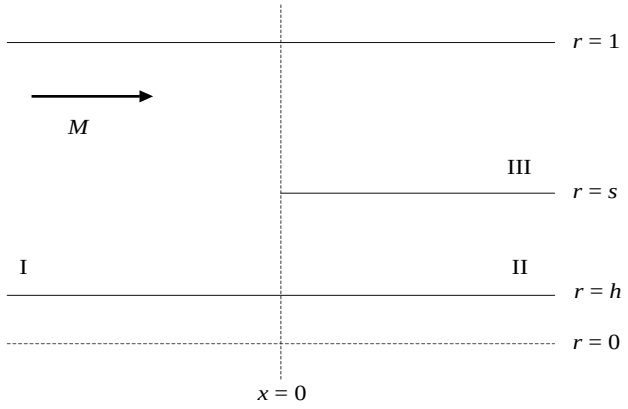


*Fig. 2 Geometry*

Under the restrictions mentioned above, and assuming small disturbances, the behaviour of the acoustic velocity potential disturbance $\phi$ is governed by the convected wave equation. Using cylindrical co-ordinates, allows separation of variables and, hence, we can consider single mode behaviour:

$$\phi(x,r,\theta,t) = \phi(r)e^{ikt+im\theta-i\alpha x}. \tag{1}$$

The values for $k$ and $m$ are fixed, which leaves the value of $\alpha$ to be found as an eigenvalue. In order to ensure the causality of the solution, the value of $k$ is considered

to be complex, $k = k_0 - i\delta$, where $k_0$ and $\delta$ are real and $0 < \delta \ll 1$. In the final solution we let $\delta \downarrow 0$.

The radial behaviour of the acoustic velocity potential disturbance is then given by Bessel functions:

$$\phi(r) = c_1 J_m(\varepsilon\, r) + c_2 Y_m(\varepsilon\, r), \tag{2}$$

with

$$\varepsilon = \sqrt{(k - M\alpha)^2 - \alpha^2}, \tag{3}$$

and where $J_m$ and $Y_m$ designate, respectively, the $m$th-order Bessel functions of the first and the second kind. It is assumed that the boundaries are hard and, hence, that the

normal component of the velocity vanishes on these boundaries. This yields the following eigenvalue equation for $\varepsilon$:

$$J'_m(\varepsilon\, a)Y'_m(\varepsilon\, b) - Y'_m(\varepsilon\, a)J'_m(\varepsilon\, b) = 0, \tag{4}$$

where the prime denotes differentiation with respect to the argument and where *(a,b) = (h,1)* for region I, *(a,b) = (h,s)* for region II, and *(a,b) = (s,1)* for region III. Equation (4) is an eigenvalue equation with solutions $\varepsilon = \varepsilon_{m\mu}$, $\mu = 1,2,3,\ldots$ Note that in the three different regions this yields three different sets $\{\varepsilon_{jm\mu}\}$, $j = 1,2,3$. The values of $\varepsilon$ correspond to values of $\alpha$ via the dispersion relation (3), which yields two values of $\alpha_{jm\mu}$ for each value of $\varepsilon_{jm\mu}$.

The total solution in each region, for fixed values of *m* and *k*, is a sum over all radial eigensolutions:

$$\phi(x,r) = \sum_{\mu=1}^{\infty} \left\{ A^+_{jm\mu} e^{-i\alpha^+_{jm\mu}x} + A^-_{jm\mu} e^{-i\alpha^-_{jm\mu}x} \right\} U_{jm\mu}(r), \tag{5}$$

where $U_{jm\mu}$ are normalised radial eigenfunctions:

$$\begin{cases} U_{1m\mu} = \left\{ J_m(\varepsilon_{1m\mu}r)Y'_m(\varepsilon_{1m\mu}h) - Y_m(\varepsilon_{1m\mu}r)J'_m(\varepsilon_{1m\mu}h) \right\} / N_{1m\mu,} \\ U_{2m\mu} = \left\{ J_m(\varepsilon_{2m\mu}r)Y'_m(\varepsilon_{2m\mu}h) - Y_m(\varepsilon_{2m\mu}r)J'_m(\varepsilon_{2m\mu}h) \right\} / N_{2m\mu,} \\ U_{3m\mu} = \left\{ J_m(\varepsilon_{3m\mu}r)Y'_m(\varepsilon_{3m\mu}) - Y_m(\varepsilon_{3m\mu}r)J'_m(\varepsilon_{3m\mu}) \right\} / N_{3m\mu,} \end{cases} \tag{6}$$

and $N_{jm\mu}$ are constants that normalise the eigenfunctions appropriately.

## DIFFRACTION PROBLEM

After the preliminary work we can use the Wiener-Hopf technique (Ref. 2) to solve the diffraction problem in the interstage region. Using the eigensolutions in the different regions of the interstage, we can write down the incoming sound waves onto the splitter. From the fan a right running wave approaches the end of the splitter:

$$R(x,r) = \sum_{\mu=1}^{\infty} B^+_{1m\mu} U_{1m\mu}(r) e^{-i\alpha^+_{1m\mu}x}, \tag{7}$$

and from the stators 'left running' waves approach the end of the splitter:

$$L(x,r)=\begin{cases}\sum_{\mu=1}^{\infty} B^{-}_{2m\mu}U_{2m\mu}(r)e^{-i\alpha^{-}_{2m\mu}x}, & h\le r\le s,\\ \sum_{\mu=1}^{\infty} B^{-}_{3m\mu}U_{3m\mu}(r)e^{-i\alpha^{-}_{3m\mu}x}, & s\le r\le 1.\end{cases} \tag{8}$$

Writing the total potential field as

$$\phi(x,r)=\psi(x,r)+R(x,r)+L(x,r), \tag{9}$$

and applying a Fourier transform in the *x* direction gives an expression for the Fourier transformed potential $\hat{\psi}$. Applying hard wall boundary conditions and continuity of the pressure at $r=s,\quad x<0,$ yields an equation in the complex *u* plane:

$$-i(k-Mu)K(u)\left(F_{-}(u)-\hat{R}_{+}(u)\right)=P_{+}(u)-\hat{L}_{-}(u), \tag{10}$$

where *u* is the Fourier co-ordinate. The functions $K,\quad \hat{R}_{+},$ and $\hat{L}_{-}$ are known, and the functions $F_{-}$ and $P_{+}$ are unknown. *K* is determined by the radial eigenfunctions in the three different regions, and $\hat{R}_{+}$ and $\hat{L}_{-}$ are integrals over the radial derivative of the right running wave and the Doppler shifted left running wave, respectively. $F_{-}$ is an integral over the radial derivative of $\psi$ and $P_{+}$ an integral over the Doppler shifted $\psi$. The latter two functions determine the solution for $\psi$. We now come to the actual application of the Wiener-Hopf technique. We define three regions in the complex *u* plane. Since $k=k_0-i\delta,$ and $0<\delta\ll 1$, there exists a $\delta_0>0$ such that $\mathrm{Im}(\alpha^{+}_{jm\mu})<-\delta_0$ and $\mathrm{Im}(\alpha^{-}_{jm\mu})>\delta_0$, for *j* = 1,2,3 and $\mu$ = 1,2,3… and $k\neq Mu$ for $|\mathrm{Im}(u)|<\delta_0$. We define the regions:

$$\begin{cases}S_{+}=\{u\mid \mathrm{Im}(u)>-\delta_0\},\\ S_{-}=\{u\mid \mathrm{Im}(u)<\delta_0\},\\ S=S_{+}\cap S_{-},\end{cases} \tag{11}$$

for which the function $\hat{R}_{+}$ is regular in $S_{+}$, the function $\hat{L}_{-}$ is regular in $S_{-}$, and the region *S* is non-empty. Since *M>0, k–Mu* is regular and non-zero in $S_{+}$. Due to causality of the solution the function $P_{+}$ is regular in $S_{+}$, and, likewise, the function $F_{-}$ is regular in $S_{-}$. The diffraction problem is solved when the kernel function *K* is split,

$$K(u)=K_{+}(u)K_{-}(u), \tag{12}$$

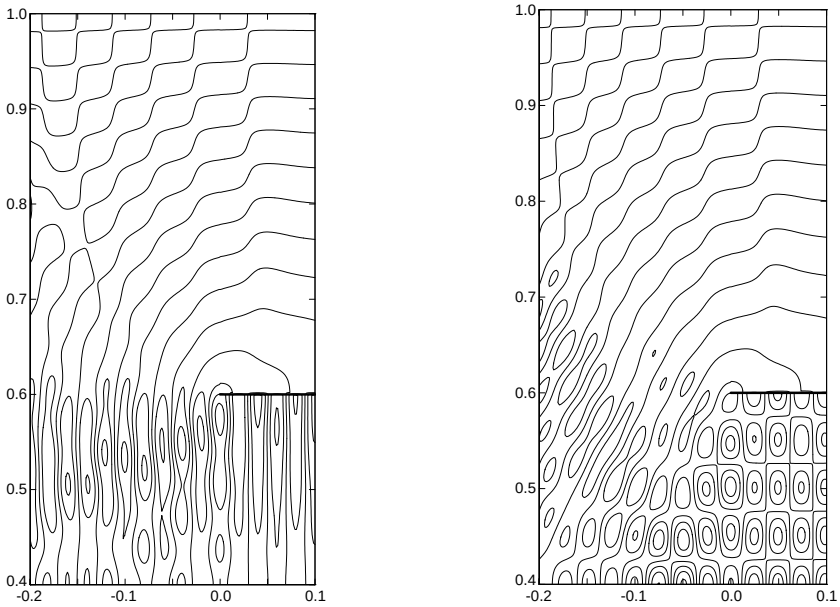


(a) (b)

*Fig. 3 (a) The first and (b) the fifth radial mode coming from the Engine Section Stators (ESS) for m=10, k=80, and M=0.5.*

such that $K_+$ is regular and non-zero in $S_+$ and $K_-$ is regular and non-zero in $S_-$. $K_+$ and $K_-$ can be found by integrating the kernel function along an appropriate path in the complex plane (Ref. 2). When the kernel function is split, equation (10) can be rewritten into an equation that has a left-hand-side that is regular in $S_-$ and a right-hand-side that is regular in $S_+$. Since $S_-$ and $S_+$ overlap, this left-hand-side and this right-hand-side define a function that is regular in *S*. This function can then be extended to a regular function in the entire complex plane. From the behaviour of this function at infinity and Liouville's theorem (Ref. 2) it follows that this function is identically zero. Hence, the aforementioned left-hand-side and right-hand-side are identically zero and from this result we can derive the solution to the diffraction problem. As an example we give the solution in region II ($x>0$, $h<r<s$):

$$\psi(x,r) = -R(x,r) - \frac{s}{2}\sum_{\mu=1}^{\infty} \frac{U_{2m\mu}(s)}{K_-(\alpha^+_{2m\mu})\sqrt{k^2-\beta^2\varepsilon^2_{2m\mu}}} \left\{ \sum_{\nu=1}^{\infty} B^+_{1m\nu} \frac{K_-(\alpha^+_{1m\nu})}{\alpha^+_{2m\mu}-\alpha^+_{1m\nu}} U'_{1m\nu}(s) \right.$$
$$+ \sum_{\nu=1}^{\infty} B^-_{2m\nu} \frac{U_{2m\nu}(s)}{K_+(\alpha^-_{2m\nu})(\alpha^+_{2m\mu}-\alpha^-_{2m\nu})} \qquad (13)$$
$$\left. - \sum_{\nu=1}^{\infty} B^-_{3m\nu} \frac{U_{3m\nu}(s)}{K_+(\alpha^-_{3m\nu})(\alpha^+_{2m\mu}-\alpha^-_{3m\nu})} \right\} U_{2m\mu}(r) e^{-i\alpha^+_{2m\mu}x}.$$

For regions I and III similar expressions are found.

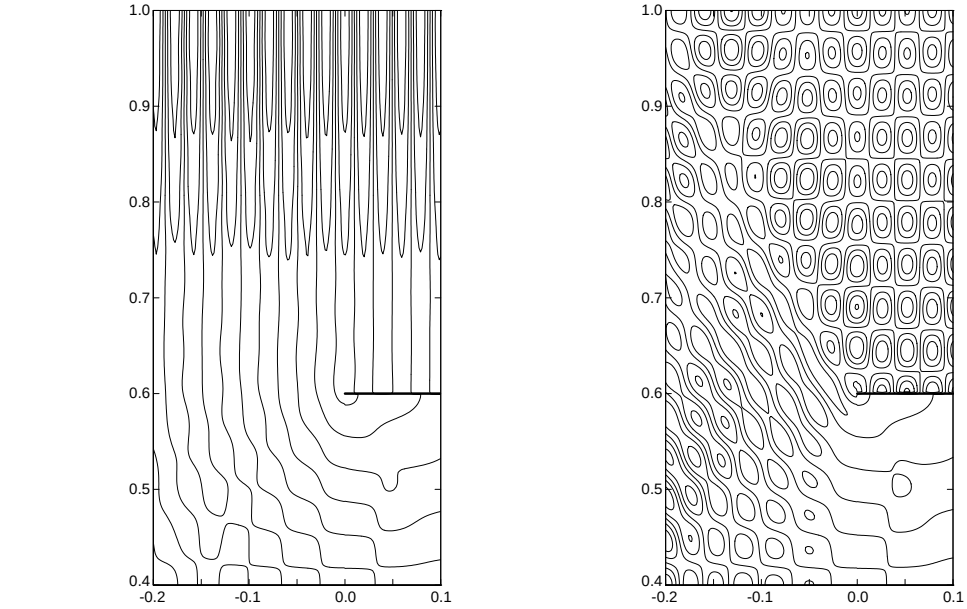


*Fig 4 (a) The first and (b) the tenth radial mode coming from the Outlet Guide Vanes (OGV) for m=10, k=80, and M=0.5.*

## RESULTS

Consider an interstage region ranging from $x = -0.2$ up to $x = 0.1$. The position of the hub is chosen to be at $r = 0.4$ and the position of the splitter at $r = 0.6$. We consider an upstream fan with *25* rotor blades and a downstream stator with *55* stator vanes. The Mach number is taken to be $M = 0.5$. Using a tip-Mach number of *0.8* for the fan, we consider a frequency $k = 80$ of four times the blade-passing frequency. For the circumferential mode number we consider $m = 10$. This results in *18* propagating modes just downstream of the fan (region I), *6* propagating modes from the ESS (region II) and *12* propagating modes from the OGV (region III). In figures 3 and 4 we show the first and fifth radial mode coming from the ESS and the first and tenth radial mode coming from the OGV. All input amplitudes are set equal to *1*. Both figures show contour plots of the total potential field $\phi$ after diffraction.

Figures 3 and 4 show that the first radial modes propagate more or less undisturbed, while the higher order modes experience more effect of the diffraction by

the end of the splitter. This effect is even stronger when the circumferential mode number is increased, but this is not shown here. Figures 3 and 4 also show that a small part of the sound is being deflected ('bends around the splitter'). In fact, also a very small part is reflected. However, most of the power reaches the trailing edge of the fan. This is shown in table 1, where the dimensionless power is shown for the original wave (input), the part that reaches the trailing edge of the fan, the part that is reflected and the part that is deflected.

| Power | input | trailing edge | reflected | deflected |
|---|---|---|---|---|
| Fig. 3a | 78.216 | 77.284 | 0.44269 | 0.48903 |
| Fig. 3b | 55.883 | 54.884 | 0.46936 | 0.52897 |
| Fig. 4a | 79.352 | 79.341 | 0.0057552 | 0.0052132 |
| Fig. 4b | 50.264 | 49.722 | 0.28815 | 0.25383 |

*Table 1 Dimensionless power for the different duct parts corresponding with figures 3 and 4*

From table 1 we see that the effect of diffraction is larger for higher order radial modes (compare Figs. 3a and 4a with Figs. 3b and 4b). Also the effect is larger for noise coming from the ESS than coming from the OGV (compare Fig. 3 with Fig. 4). This may be explained by the fact that the radial eigenfunctions have smaller amplitude at a lower radial position, which becomes more distinct at higher radial order.

Although almost all the power reaches the fan, the distribution of radial modes has changed by the diffraction. This is especially true for the higher order radial modes. Due to this different distribution, the blockage of the noise by the fan may be different, hence, resulting in different noise levels ahead of the fan. To illustrate this effect we performed some rotor blockage calculations (see Ref. 3), the results of which are shown in table 2.

| Power | Fig. 3a | Fig. 3b | Fig. 4a | Fig. 4b |
|---|---|---|---|---|
| no splitter | 69.750 | 56.400 | 21.470 | 6.428 |
| splitter | 62.904 | 12.542 | 21.307 | 12.728 |
| difference | 0.446 dB | 6.529 dB | 0.033 dB | -2.967 dB |

*Table 2 Dimensionless power after rotor blockage and difference between splitter and no-splitter case expressed in dB*

In table 2 the dimensionless power after rotor blockage is shown for situations corresponding with figures 3 and 4. When no splitter is considered, the inner duct and

the outer duct are treated as separate ducts, also ahead of the fan. For these calculations we used the power input levels of table 1. When the splitter is taken into account, the same input levels are used, but first the effect of diffraction is calculated. This means that only the power that reaches the fan (see table 1) is used for the blockage calculations. In this case the fan blocks the noise coming from the stators and has a larger effect than reflection by the splitter. However, the redistribution of power over the radial modes by the splitter makes that the power level after rotor blockage may decrease or increase when comparing the splitter case with the no-splitter case. An explanation for this may be the fact that the fan blocks the noise better at larger radial positions than at lower radial positions. Although for general wave packages the effect of the splitter on rotor blockage calculations is unpredictable, it is clear that the effect of splitter diffraction is important for a realistic modelling of turbofan engine noise.

## CONCLUSIONS

The diffraction model presented here leads to a better description of noise propagation in the interstage region of a turbofan engine. For the solution of the diffraction problem the Wiener-Hopf technique is used, which yields a closed form solution. For a given geometry, modal structure, and input amplitudes, output amplitudes are generated. The model was applied to realistic turbofan configurations.

It was found that the effect of diffraction is larger on higher order radial modes than on lower order radial modes. Also diffraction effects are more important for noise coming from the ESS than for noise coming from the OGV.

At the frequency considered, the level of noise being reflected at the edge of the splitter and bending back from ESS to OGV (or from OGV to ESS) is small as compared to the level of noise propagating forward. However, due to diffraction a redistribution of noise over the radial modes takes place. This redistribution has major implications for the effect of rotor blockage.

## ACKNOWLEDGEMENTS

This investigation has been carried out within the Brite/Euram project RESOUND. Fruitful discussions with J.B.H.M. Schulten are gratefully acknowledged.

REFERENCES

1. Sijtsma, P.; Rademaker, E.R.; Schulten, J.B.H.M.; *Experimental validation of lifting surface theory for rotor-stator interaction noise generation,* AIAA Journal, **36** (1998), 900-906.
2. Noble, B.; *Methods based on the Wiener-Hopf technique for the solution of partial differential equations*, Pergamon Press, 1958.
3. Schulten, J.B.H.M.; *Sound transmission through a rotor*, Proceedings *DGLR/AIAA* 14th Aeroacoustics Conference (Aachen, Germany), Vol. I, Deutsche Gesellschaft für Luft- und Raumfahrt, Bonn, Germany, 1992, pp. 502-509.